applied sciences

MDPI

Article

Innovative Tool to Determine Radiative Heat Transfer Inside Spherical Segments

Joseph Cabeza-Lainez

Department of Architectural Composition, University of Seville, Av. Reina Mercedes 2, 41012 Sevilla, Spain; crowley@us.es

Featured Application: Radiative form factor calculations without integrals.

Abstract: The classic equations used to find the form factor inside fragments of spheres are often unassailable. The main difficulties that they present lie in iterative integrations effected over curved surfaces. The typical simulation software for this kind of issue is not capable of tackling the drawbacks that appear in the process, among them we could cite the impossibility of discretizing curved shapes with equal matching tiles, whether triangles or rectangles, especially when we arrive at the contour elements. The current type of cylindrical tiles employed for the calculation of spheres, due to incoherence in curvature, presents a significant array of gaps that render the whole procedure inadequate and inconsistent. To countermeasure this drawback, the recent finding of some innovative principles by the present author has provided a sure and exact path towards the solution of the problem in the frequent case of a volume enclosed within a spherical fragment and two limiting sections of the said sphere placed at arbitrary positions. The coherent application of such postulates by virtue of form factor algebra leads to an encompassing expression which solely requires the input of the surface areas of the involved shapes and, thus, avoids the lengthy resort to integration. A relevant number of cases in radiative heat transfer simulation, that cannot be solved by any other method, become feasible and accurate. Since the new tool can be implemented as an algorithm for simulation software, pivotal advances emerge in the complex domain of radiation which are applicable for the lighting industry, building simulations, and aerospace technologies, among others.

Keywords: radiative heat transfer; form factor calculation tools; spherical geometry; design of LED sources

Citation: Cabeza-Lainez, J. Innovative Tool to Determine Radiative Heat Transfer Inside Spherical Segments. *Appl. Sci.* **2023**, *13*, 8251. https://doi.org/10.3390/app13148251

Academic Editors: Lioua Kolsi, Walid Hassen and Patrice Estellé

Received: 13 June 2023
Revised: 6 July 2023
Accepted: 15 July 2023
Published: 16 July 2023

1. Introduction

View or form factors are a relevant entity in all the phenomena that involve radiation [1]. Since this particular process of heat transfer, unlike the common belief, does not imply any kind of continuity or contact between the affected bodies, pure form and position become pivotal for the transmission of energy [2]. Diffuse radiation is inextricably correlated to surface area [3]. In basic elementary shapes (cuboid), no particular problem appears with such a concept [3], but when it is required to extend the well-known differential equations to concrete and finite forms arbitrarily deployed, we have to deal with two sets of different and often complex double integrals [4,5]. It is known that to obtain an exact fourfold primitive, even of the simplest elements, is a mathematical feat and often a serendipity, to say the least [6].

Even recent studies have failed to overcome this severe hindrance for the completion of important problems in radiative transfer in the void [3]. Experts have frequently resorted to numerical or statistical approaches such as Monte Carlo methods [7], albeit they are not conclusive in most cases, not only because of the many errors that arise in the process but also due to the impossibility of validating their accuracy as they are in fact the only method available to try to surmount this shortcoming. In the case that we are addressing, Monte

Carlo methods are not available due to the presence of double curvatures which invalidate any form of regular or coherent tiling of the surfaces.

The present author was able to perform the said quadruple integration in an exact manner solely for three kinds of simple forms: rectangles (whether perpendicular or parallel), parallel coaxial circles, and the same for a sphere and a circle [8,9]. It seems puzzling that if the rectangles simply form an angle different to $\pi/2$ or zero between them, or if the circles are slightly offset or placed in a perpendicular fashion, we cannot even reach an exact solution to the problem of finding the form factor between these rather common elements.

If the forms are incomplete and fragmented, then the problem increases significantly because we need to remark that, until the author discovered it, there was no exact solution available even for the form factor due to a triangle [10]. Only the simpler expression of the configuration factor (a double integral entity which regulates the exchange on a point to point basis, but not including the whole surface) had been identified and solved for particular points [11].

Furthermore, another degree of complexity arises when the exchanges take place in a three-dimensional environment or in other words, the surfaces involved are not planar but curved or warped [12].

It is clearly improbable for the time being to find the form factor of a set of arbitrarily curved surfaces by integration alone [3]. However, other numerical methods based on discretization of the said areas in differential units are also not viable since such kinds of surfaces cannot be divided into any form of regular, concentric, or symmetrically patterned tiles. Once again we arrive at the previous impasse. With enough fortune and considerable effort, the author has discovered ways to advance in the finding of exact solutions by means of innovative principles of their own creation [13], suitable for algebraic treatment and eventually offering exact expressions that altogether avoid integration and are currently being programmed in algorithms. In the following sections we will explain and develop one such property, perhaps the most relevant of all.

2. Materials and Methods—General Departing Equation

The canonical equation that regulates a general exchange of radiant energy for arbitrary and non-planar surfaces, as depicted in Figure 1, can be written in the following form (Equation (1)):

$$d\phi_{12} = (E_1 - E_2)\cos\theta_1 \cos\theta_2 \frac{dA_1 dA_2}{\pi r_{12}^2} \quad (1)$$

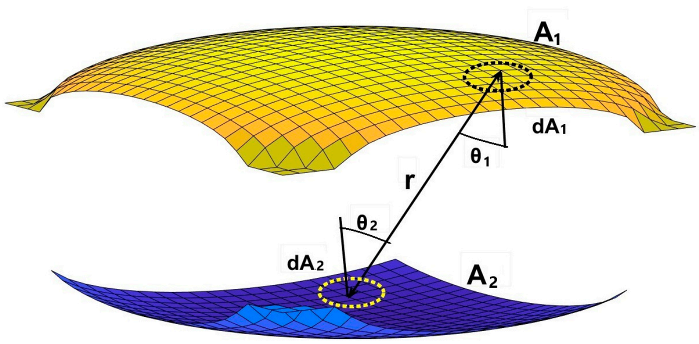

Figure 1. Radiation interchanges for a set of arbitrary curved surfaces, called A_1 and A_2.

Equation (1) derives from the reciprocity theorem first stated by Lambert [14–16] and it gives the rate of diffuse radiant energy, in W/m^2, that is transmitted into the void from each of the surfaces, namely, E_1 and E_2. The angles θ_1 and θ_2 are formed between the normal and the respective surfaces and the segment that links any arbitrary couple of points termed r_{ij} (see nomenclature).

Thorough solving of Equation (1) implies four rounds of integration [4]. The present author has been able to finish them with much difficulty for the following shapes: perpendicular rectangles with a common edge, parallel rectangles, parallel coaxial disks, and a parallel coaxial circle under a sphere [8]. The last two are possible since the polar coordinates coincide for the involved coaxial elements. Other authors have reported a similar solution but they have not fully demonstrated their integral procedures [16–18], and some of them seem inconclusive or incomplete although they are frequently quoted [19–21].

For other different positions of the surface sources, an exact solution has not been achieved yet [5]. Neither for triangles or irregular fragments of rectangles and circles or even for the familiar form of the sphere.

Intermediate steps to proceed only with the first and the second round of integration have been proposed [22]. They usually end at a single point or elementary area that belongs to the receiving surface. Some of them are recorded under the misleading manner of nomograms at catalogues of radiation view factors [23,24]. Such results are somewhat helpful but they are by no means general and can be confusing in many situations.

Subsequently, if we try to apply the former calculations to the interior of a sphere, we can identify two important postulates for this domain.

To begin with, suppose for instance that the fragment under study is a simple hemisphere (Figure 2), in this situation the half-sphere encloses a space made of two surfaces, that is, a cap and a circular base [25]. Their respective areas amount to $A_1 = 2\pi R^2$ (cap) and $A_2 = \pi R^2$ (disk). Under such circumstances, it is not feasible to extend double integration to the disk and the hemisphere at the same time, or at least not in the way that we would apply for parallel rectangles running only through coordinates x and y, because Cartesian coordinates are interchangeable and polar coordinates are not, since they need to originate from the same central point and that makes them unmanageable. However, by the principle of conservation of energy, we know that all radiant interchanges inside a closed volume must add to 100% or the unity [6]. Thus, the orderly array of form factor algebra for the two surfaces implies,

$$F_{11} + F_{12} = 1; \tag{2}$$

$$F_{21} + F_{22} = 1. \tag{3}$$

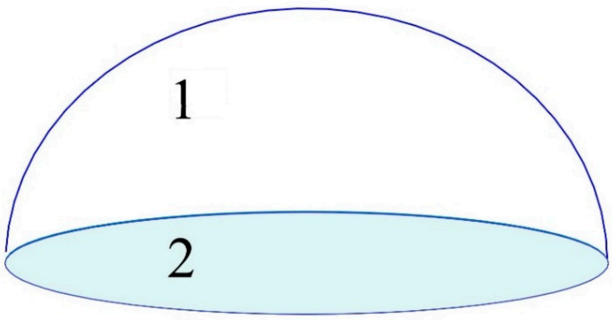

Figure 2. Form factor calculation applied to a hemisphere, Surf. 1 (eq: $x^2 + y^2 + z^2 = R^2$, with origin at 0,0,0) with a circular base, Surf. 2 (eq: $x^2 + y^2 = R^2$) at the same origin.

However, the disk is planar, and in Equation (3) we know that F_{22} equates to zero. Thus, F_{21} must be one in order to fulfil the equation.

By the reciprocity theorem mentioned in Equation (1), and the said algebra, we also obtain

$$A_2F_{21} = A_1F_{12}; \tag{4}$$

$$F_{12} = A_2/A_1F_{21}; \tag{5}$$

with this, F_{12} needs to be 1/2 and so $F_{11} = 1/2$.

An unexpected fact has happened in front of our eyes. The appearance of the former result implies that the amount of energy diffusely radiated from the hemisphere to itself or F_{11} has a definite value, other than null, and the highest probability of particles reaching the emitting source is equal to the area of the same fragment of the sphere divided by the total extension of the theoretical complete sphere, $4\pi R^2$ (Figure 3). Unlike planar surfaces, their curved counterparts present the rare property of "seeing" themselves under radiative fields as a result of their own curvature. Such a relevant geometric fact has been largely ignored in the heat transfer literature. Nonetheless, the author has demonstrated that the said relationship holds true for all kind of fragments of sphere regardless of their size or relative position within the surface [26].

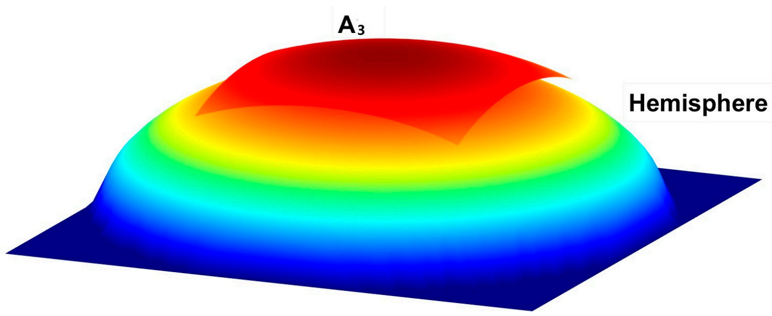

Figure 3. Half-sphere with outlined section of sphere A_3 in red mapping, which is employed to account for the finding of F_{33}, or the form factor of the section over itself (color codes selected for clearer visualization).

Becoming an invariable and significant relationship, previously unknown, such a finding has been named Cabeza-Lainez's first principle.

From Figure 3, it can be expressed algebraically as a simple ratio which gives the maximum probability of energy attainment in this configuration (Equation (6)) [27]:

$$F_{33} = \frac{A_3}{A_s} = \frac{A_3}{4\pi R^2} \tag{6}$$

The second form factor given in Equation (5), namely, $F_{12} = A_2/A_1 = 1/2$, amounts to the ratio between the area of the disk and that of the enclosing surface (the cap). This represent the maximum theoretical probability for the quanta of energy from the covering source to reach the base circle. In this case, the previous invariance property applies to any arbitrary surface that surrounds the circle entirely and not just to the spherical cap (Figure 4). Accordingly, it is called the second postulate of radiant energy of Cabeza-Lainez.

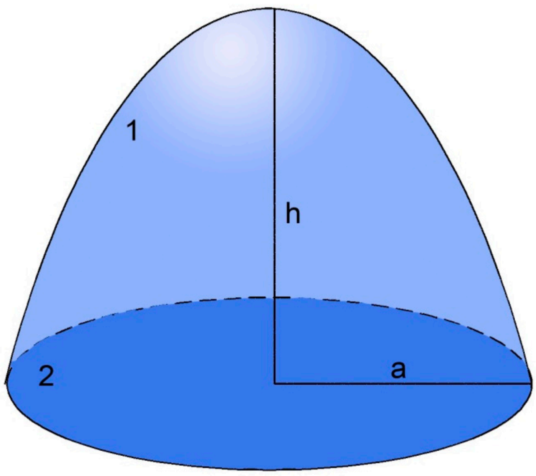

Figure 4. A circular disk of radius a (surf. 2) topped by a paraboloid of height h (surf. 1), used to illustrate the invariance of Cabeza-Lainez's second postulate.

3. Results

Let us now apply the previous findings to the problems of exchange in the interior of a sphere. To this aim, consider a volume formed by three surfaces (Figure 5), a fragment of a sphere (surface 3), and two limiting planar elements (areas 1 and 2).

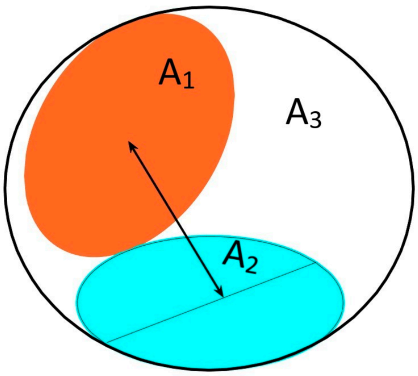

Figure 5. The three surfaces appearing in radiative exchanges for the inside of a sphere. Two planar sections (not necessarily circular nor equal) and a spherical fragment as an enclosure.

The form factor algebra demonstrated in references [1,5,12,17] gives that,

$$F_{11} + F_{12} + F_{13} + \ldots\ F_{1N} = 1 \quad (7)$$

As defined in the first principle (Equation (6)), F_{33} stands for the relation between the areas of the spherical section (however irregular in shape) and the total area of the sphere, to which surface 3 pertains. F_{33} is, in this way, constant for any derived surface as far as it belongs to the enveloping sphere [22].

In this case, if we use the previous algebra (Equation (7)) to solve the remaining factors, we will obtain the following system of three equations:

$$F_{12} + F_{13} = 1; \quad (8)$$

$$F_{21} + F_{23} = 1; \quad (9)$$

$$F_{31} + F_{32} + F_{33} = 1. \quad (10)$$

Remembering that, as the planar surfaces 1 and 2 do not “see” each other in the radiation field, there is neither F_{11} nor F_{22} in this set of equations as they amount to zero.

Consequently,

$$F_{12} = 1 - F_{13}; \quad (11)$$

$$F_{13} = 1 - F_{12}; \quad (12)$$

$$F_{23} = 1 - F_{21}. \quad (13)$$

However, the reciprocity theorem [3] implies that:

$$A_3F_{32} = A_2F_{23} \quad (14)$$

Thus, successively,

$$F_{32} = \frac{A_2}{A_3}(1 - F_{21}); \quad (15)$$

$$F_{31} = \frac{A_1}{A_3}(1 - F_{12}). \quad (16)$$

From Equation (10), we know that

$$F_{31} = 1 - F_{32} - F_{33}. \quad (17)$$

Substituting (15) and (16) into (17),

$$\frac{A_1}{A_3}(1 - F_{12}) = 1 - \frac{A_2}{A_3}(1 - F_{21}) - F_{33}. \quad (18)$$

Additionally, by changing F_{21} to its reciprocal F_{12} in Equation (18):

$$\frac{A_1}{A_3}(1 - F_{12}) = 1 - \frac{A_2}{A_3} + \frac{A_1F_{12}}{A_3} - F_{33}. \quad (19)$$

In turn, multiplying both terms by A_3, we would obtain

$$A_1 - A_1F_{12} = A_3 - A_2 + A_1F_{12} - A_3F_{33}. \quad (20)$$

Additionally, simplifying,

$$2A_1F_{12} = A_1 + A_2 - A_3 + A_3F_{33}. \quad (21)$$

Thus, working out F_{12}, Equation (21) yields,

$$F_{12} = \frac{1}{2}\left(1 + \frac{A_2 - A_3}{A_1} + \frac{A_3}{A_1}F_{33}\right). \quad (22)$$

Formerly, this equation would have remained unresolved, but thanks to the patient research embodied in Cabeza-Lainez’s first principle we are in the position of substituting F_{33}, equal to A_3/A_s, from Equation (6) and attaining, for the first time, a physical solution to the problem and a major finding that encompasses many other unaffordable problems.

Then, Equation (22) is completely solved with perfect ease. The exchange of energy for any couple of surfaces that enclose an arbitrary spherical fragment is found as,

$$F_{12} = \frac{1}{2}\left(1 + \frac{A_2 - A_3}{A_1} + \frac{A_3A_3}{A_1A_s}\right). \quad (23)$$

Derived from Equation (23), Cabeza-Lainez's third postulate gives,

$$F_{12} = \frac{1}{2}\left(1 + \frac{A_2 - A_3}{A_1} + \frac{A_3^2}{A_1 A_s}\right). \quad (24)$$

Only the areas of the three involved surfaces plus that of the complete sphere appear in this expression. The problem of finding the radiative exchanges inside the volume composed of three curved figures is completely solved in an elegant manner without resorting to integration.

The finding of the areas for 1 and 2 is normally simple, but determining the lateral area of the sectioned sphere may require managing a special kind of trigonometry and the curved angles that appear in it. The theorem of Girard [28] is often useful for this task. In the first example proposed, the planar figures possess a common tangent point, but this is not necessary in all cases as the postulate is perfectly general. In fact, the sections of the sphere can be detached, connected, or intersected as in the case of two semicircles. Surfaces 1 and 2 can be different in size and shape, as determined by the enveloping sphere [29].

The rest of the factors required in the calculation, F_{13}, F_{21}, F_{23}, F_{31}, and F_{32} can be found without difficulty from Equations (11)–(16).

For example,

$$F_{13} = 1 - \frac{1}{2}\left(\frac{A_1 + A_2 - A_3}{A_1} + \frac{A_3^2}{A_1 A_s}\right) = \frac{1}{2} - \left(\frac{A_2 - A_3}{2A_1} + \frac{A_3^2}{2A_1 A_s}\right); \quad (25)$$

$$F_{31} = \frac{A_1}{2A_3} - \left(\frac{A_2 - A_3}{2A_3} + \frac{A_3^2}{2A_3 A_s}\right) = \frac{A_1}{2A_3} - \left(\frac{A_2 - A_3}{2A_3} + \frac{A_3}{2A_s}\right); \quad (26)$$

$$F_{21} = \frac{A_1}{2A_2}\left(\frac{A_1 + A_2 - A_3}{A_1} + \frac{A_3^2}{A_1 A_s}\right) = \frac{A_1 + A_2 - A_3}{2A_2} + \frac{A_3^2}{2A_2 A_s}; \quad (27)$$

$$F_{23} = 1 - \frac{A_1 + A_2 - A_3}{2A_2} - \frac{A_3^2}{2A_2 A_s} = \frac{1}{2} - \left(\frac{A_1 - A_3}{2A_2} + \frac{A_3^2}{2A_2 A_s}\right). \quad (28)$$

4. Discussion

To continue, we will discuss in this section, the applicability of the results derived from the new form factor equations for several usual configurations.

In the first place, we will study the expressions deduced in Equations (24)–(28) for a new case of two tangent circles which form an arbitrary angle from 0 to π (Figure 6). If the surfaces A_1 and A_2 are equal, the postulate reduces to

$$F_{12} = \frac{2A_1 + A_3(F_{33} - 1)}{2A_1} = \frac{1}{2}\left(\frac{2A_1 - A_3}{A_1} + \frac{A_3^2}{A_s A_1}\right) = 1 + \frac{A_3}{2A_1}\left(\frac{A_3}{A_s} - 1\right) \quad (29)$$

$$F_{13} = \frac{A_3}{2A_1}\left(1 - \frac{A_3}{A_s}\right) \quad (30)$$

Should the angle between the said circles stand at $\pi/2$ (perpendicular), by common geometry rules we can substitute the respective values of the magnitudes in Equation (25) to obtain F_{12}.

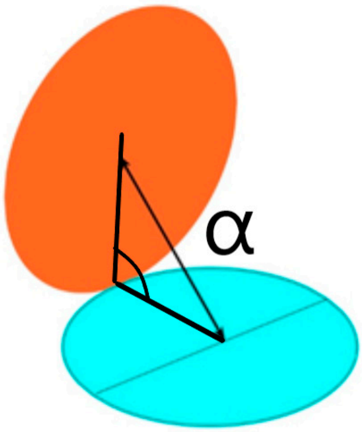

Figure 6. Form factor calculation between two circles with a tangent point forming an arbitrary angle α.

The area of the two equal circles $A_1 = A_2$ is $\pi R^2/2$, the former Equation (29) can then be cleared to

$$F_{12} = 1 + \frac{A_3(F_{33} - 1)}{\pi R^2} = 1 + \frac{A_3^2}{A_s \pi R^2} - \frac{A_3}{\pi R^2} \tag{31}$$

A_3 is obtained as the total area of the sphere, $4\pi R^2$, minus two spherical segments whose lateral area equates to $\pi(a^2 + h^2)$, where a represents half of the base of the segment and h is the perpendicular distance from the base to the top of the segment.

Therefore, by simple trigonometry, h is $R(1-\sqrt{2}/2)$ and a equates to $R\sqrt{2}/2$.

$$a^2 = \frac{R^2}{2};\ h^2 = R^2\left(\frac{3}{2} - \sqrt{2}\right) = \frac{R^2}{2}\left(3 - 2\sqrt{2}\right) \tag{32}$$

$$a^2 + h^2 = \frac{R^2}{2}\left(4 - 2\sqrt{2}\right)$$

$$A_3 = 4\pi R^2 - 2\pi\frac{R^2}{2}\left(1 + 3 - 2\sqrt{2}\right) = 4\pi R^2 - 2\pi R^2\left(2 - \sqrt{2}\right) = \pi R^2 2\sqrt{2} \tag{33}$$

Squaring this area in accordance, we obtain,

$$A_3^2 = 8\pi^2 R^4 \tag{34}$$

Substituting into Equation (29),

$$F_{12} = 1 + \frac{8\pi^2 R^4}{4\pi R^2 \pi R^2} - \frac{\pi R^2\left(2\sqrt{2}\right)}{\pi R^2} \tag{35}$$

Thus, the sought factor F_{12} is obtained as

$$F_{12} = 1 + 2 - 2\sqrt{2} = 3 - 2\sqrt{2} = 0.1715 \tag{36}$$

For a general case of any subtended angle $\alpha = 2\theta$, the area of the circles as compared to the sphere yields

$$A_1 = A_2 = \pi R^2 \cos^2\theta \tag{37}$$

To compare with the above perpendicular case, remember that $\cos\theta$ was there equal to $\cos(\pi/4) = \sqrt{2}/2$, and $A_1 = A_2 = \pi R^2/2$.

In this more encompassing case, the spherical caps resulting from the limit sections, present the parameters $a = R/2 \cos\theta$ and $h = R(1 - \sin\theta)$.

Therefore, if we subtract the area of those caps from the total area of the sphere, A_3 is equal to $4\pi R^2 \sin\theta$, F_{33} gives $\sin\theta$, Equation (28) is adapted accordingly and the entirely new form factor yields, after considerable manipulation,

$$F_{12} = 1 + \frac{2\sin\theta(\sin\theta - 1)}{\cos^2\theta} = F_{21} = 1 + \frac{2\sin^2\theta - 2\sin\theta}{1 - \sin^2\theta} \tag{38}$$

Or writing it in terms of the double angle α,

$$F_{12} = 1 + 2\sin\frac{\alpha}{2}\left(\sin\frac{\alpha}{2} - 1\right) / \cos^2\frac{\alpha}{2} \tag{39}$$

This represents a totally new postulate to determine the form factor between tangent circles that form any angle from 0 to π. It is an undeniable finding. The value of the curve for $\alpha = \pi/2$ is 0.17, as found previously in Equation (43). Such a curve has been named "Herodias" by the author. It is represented in Figure 7.

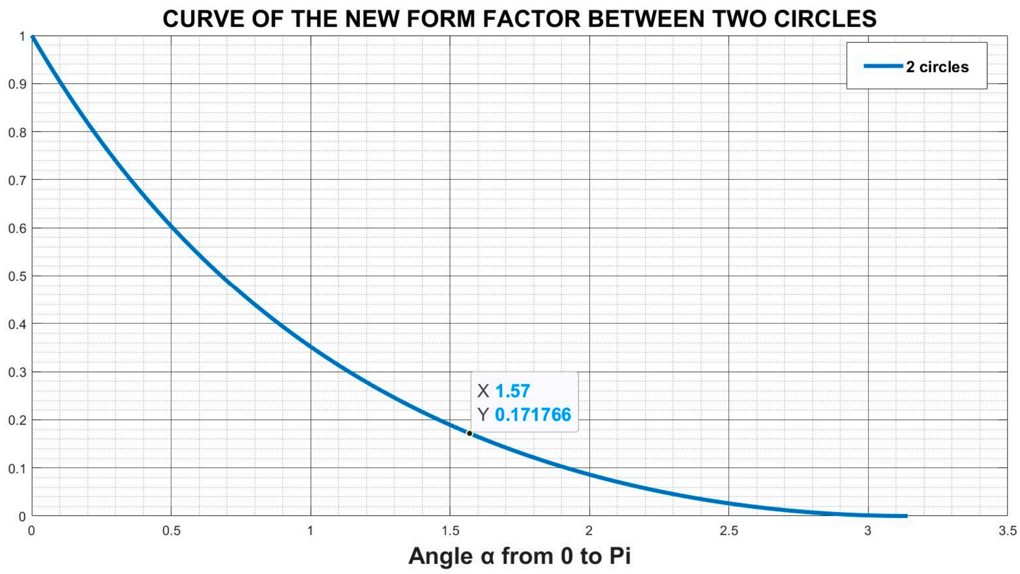

Figure 7. Form factor calculation between two circles with a tangent point forming an arbitrary angle.

Other important form factors that are obtained from Equation (36) are those of F_{13} and F_{31},

$$F_{13} = \frac{2\sin\theta(1 - \sin\theta)}{\cos^2\theta} = F_{23} \tag{40}$$

$$F_{31} = \frac{1 - \sin\theta}{2} = F_{32} \tag{41}$$

with which we confirm that some of the expressions found are as simple as they are elegant.

A second discussion case, inspired by the first, deals with two semicircles which share a common edge. In this case the symmetric planar sections start at the center of the containing sphere, while in case 1 they departed from a pole or extreme of the said sphere.

The author could obtain by deduction the form factor due to half-disks of identical radius R with a shared straight edge, as a function of the subtended angle α between the semicircles. From there, the corresponding factors with the surrounding fragment of the sphere are obtained [9] and are considered innovative and important contributions of the author [13,29,30] (Figure 8).

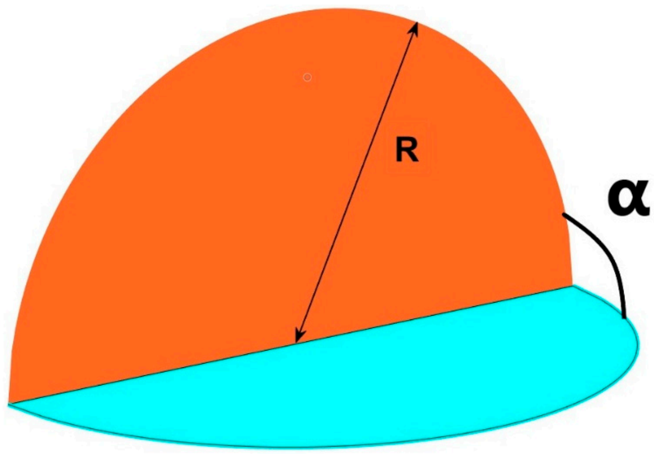

Figure 8. Two half-disks of identical radius R with a shared linear border and forming the internal angle α.

Under that situation, the solving equation is based on angles only,

$$F_{12} = 1 - \frac{2\alpha}{\pi} + \left(\frac{\alpha}{\pi}\right)^2 \tag{42}$$

Introducing the parameter p,

$$p = \frac{\alpha}{\pi}$$

We can simplify the former equation which appears in Figure 9 as:

$$F_{12} = 1 - 2p + p^2 = F_{21} \tag{43}$$

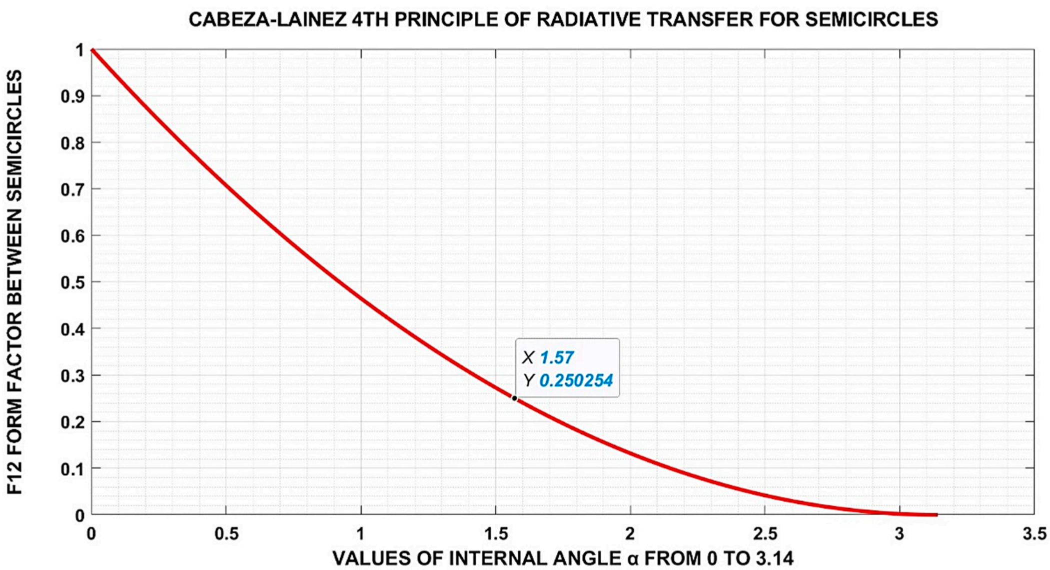

Figure 9. Graph of the equation of Cabeza-Lainez's fifth postulate (Equation (42)) which gives the factor for half-disks, note the abscissa for the angle = $\pi/2$ = 1.57 which is 0.25.

Accordingly, we present the expressions for F_{13} and F_{31}:

$$F_{13} = \frac{2\alpha}{\pi} - \left(\frac{\alpha}{\pi}\right)^2 \tag{44}$$

$$F_{31} = 1 - \frac{\alpha}{2\pi} \tag{45}$$

While the formulation of such a new factor can be regarded as something evident, we need to notice that it is unfeasible to find it by any other procedure [31,32]. For instance, detailing the contour integral calculation for an angle of $\pi/2$ (Figure 10), it is understood that it would be too complex, and in fact the author has not been able to solve it beyond the third round of integration (Equation (45)).

$$F_{12} = \int_0^{\pi}\int_0^{\pi}\int_0^{R}\int_0^{R} \frac{(r_1^2 r_2 \sin\theta_1 r_2^2 r_1 \sin\theta_2) dr_1 dr_2 d\theta_1 d\theta_2}{\pi * \left[(r_1^2 + r_2^2 + 2r_1 r_2 \cos\theta_1 \cos\theta_2)\right]^2} = 1/4 \tag{46}$$

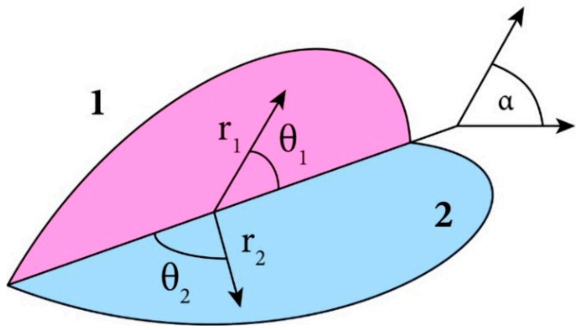

Figure 10. Radiant exchange between the conjugate disks cutting at a shared edge under a variable angle α.

The expression found in Equation (46), which is solely valid for $\alpha = \pi/2$, denotes the extreme difficulty of the form factor F_{12} in this configuration and is subsequently used to determine the radiant emissions that take place in Figures 8 and 10. Such energy flux formulas are impractical to obtain in an accurate fashion for the perpendicular position, let alone different tilts of the involved surfaces [33–35]. Consequently, this postulate, number five, can be seen as a meaningful contribution. Furthermore, it is completely incardinated in the third postulate explained in the results section and it can be considered as a particular, simpler case of the more general one [36].

In Figure 11, there is a graph of comparison of the values for the fourth and fifth postulates. They both go from 0 to 1 in magnitude but the factor corresponding to two semicircles is slightly higher at all angles than the one found for the complete circles and this can be attributed to the different arrangement of the surfaces in space [37]. In a word, the half-disks lie in closer proximity than the circles.

In a manner of validation, we can calculate the form factor for different spherical wedges, namely, the octave and the quarter of a sphere.

The area of any wedge of a sphere depends on the angle it covers and is defined as $A_3 = 2\alpha R^2$, where α is the angle already stated between two semicircles which share an edge at the center of the sphere. For the whole surface, $\alpha = 2\pi$.

In this case, an eighth gives, $\alpha = 2\pi/8 = \pi/4$ and then $A_3 = \pi R^2/2$.

However, we know by virtue of Cabeza-Lainez's first principle [5], explained in Section 2 of the article, that $F_{33} = \frac{\pi R^2/2}{4\pi R^2} = \frac{1}{8}$.

That fraction represents the area of an eighth of the sphere over the total area.

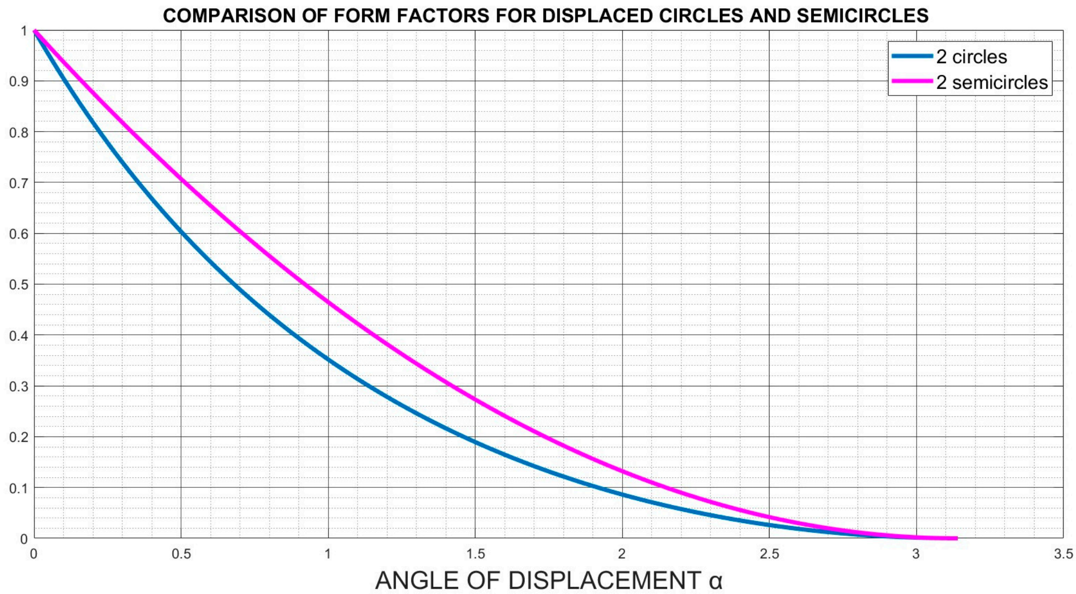

Figure 11. Comparison of the radiative exchange between two circles and two semicircles rotated in an angle α from 0 to π.

Moreover, using the third postulate in this specific case, from Equation (29),

$$F_{12} = \frac{2A_1 + A_3(F_{33} - 1)}{2A_1} = \frac{\pi R^2 + \pi R^2/2(1/8 - 1)}{\pi R^2} = 1 - \frac{7}{16} = \frac{9}{16} = 0.5625 \quad (47)$$

In order to obtain the previous result, we need to remember that $A_1 = A_2 = \pi R^2/2$ and consequently both areas are the same and so is A_3 (Equation (47)).

This coincides with the cypher deduced from Cabeza-Lainez's fifth principle, as in such a formulation we would have arrived at the following for $\alpha = \pi/4$ (Equation (42)),

$$F_{12} = 1 - \frac{1}{2} + \left(\frac{1}{4}\right)^2 = \frac{1}{2} + \frac{1}{16} = \frac{9}{16} = 0.5625 \quad (48)$$

Subsequently, if we apply the same deduction to the quarter of a sphere, we would obtain that,

$$F_{12} = \frac{A_1 + A_2 + A_3(F_{33} - 1)}{2A_1} = \frac{\pi R^2 + \pi R^2(1/4 - 1)}{\pi R^2} = 1 - \frac{3}{4} = \frac{1}{4} = 0.25 \quad (49)$$

Which is pointed out in the graph of Figure 9 for the angle $\pi/2$.

With both surfaces being perpendicular the former value has been checked by the author by means of a novel numerical method. In ref. [2], the author demonstrated that the form factor entity between any set of two surfaces equates to the mean value of the point to point view factor distributed over the receiving element [32]. Such a procedure was employed to validate the quantity of 0.25 referred to above and other complex situations have also been analyzed with the same approach.

As an example, for the perpendicular semicircles with the same radius described in Figure 8, the said value of 0.2504 has been determined by means of our graphical–numerical method performed in Matlab (Figure 12).

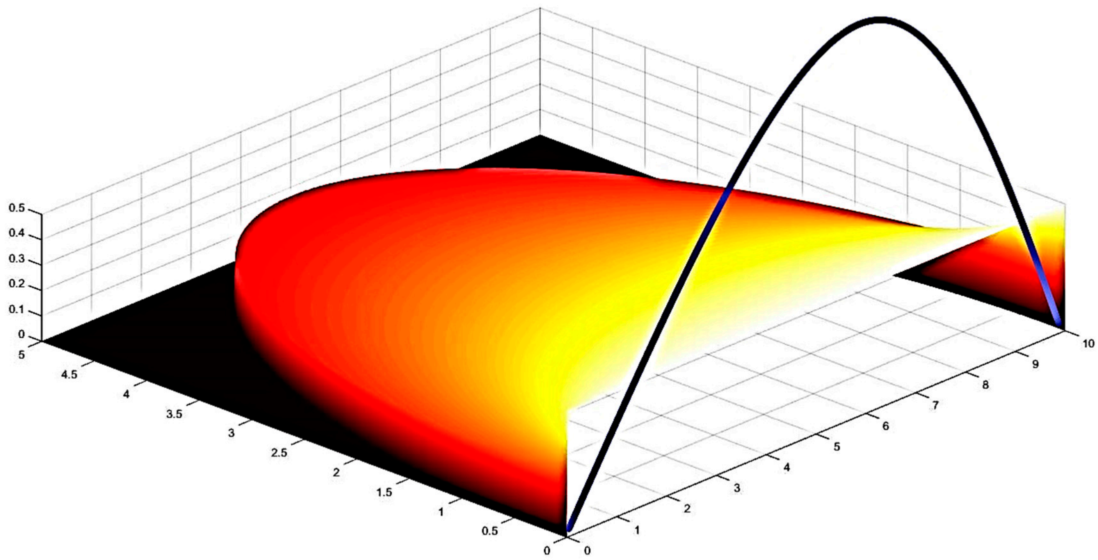

Figure 12. Three-dimensional view of the numerical calculation performed by Matlab on the configuration factor from a semicircle over its perpendicular counterpart.

To apply the principles explained, we present the case of a famous building where these two semicircles appear, the so-called Scenic Triclinium of Hadrians' Villa near Rome (Figures 13 and 14).

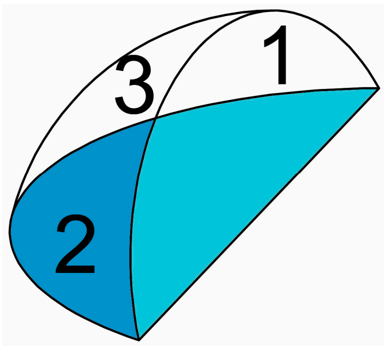

Figure 13. The two limiting semicircles 1 and 2 (eqs. $x^2 + y^2 = R^2$ and $x^2 + z^2 = R^2$) that enclose the half dome 3, which appears at the Scenic Triclinium in Tivoli (Rome).

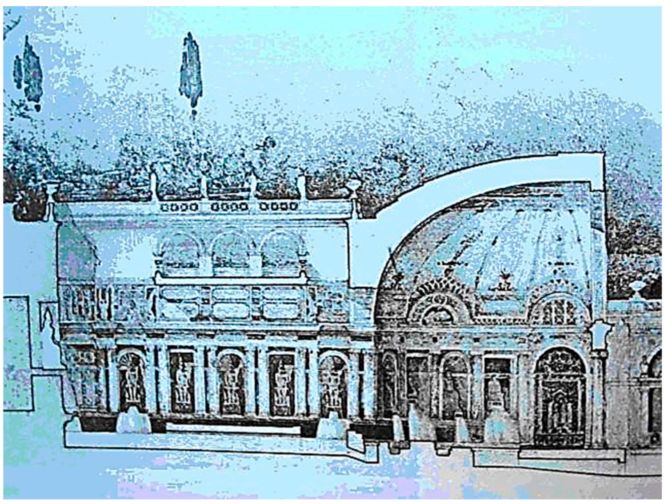

Figure 14. Archaeological section of the Scenic Triclinium in Tivoli.

By means of the fourth postulate hereby deduced, calculations of the reflected energy transmitted to the ground level have been effected by the author (Figure 15).

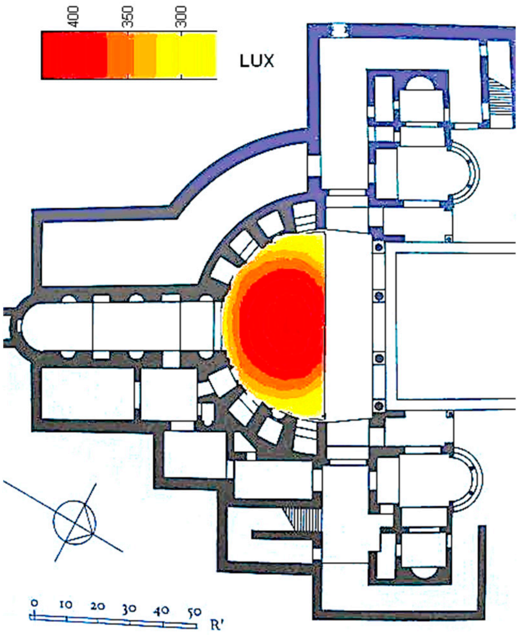

Figure 15. Distribution of radiant energy under the dome of the Triclinium attributed to the arched aperture during June's solstice.

As a concluding remark, we need to stress that due to the author's original formulation, the limiting surfaces to the spherical segment do not need to be equal [38–40]. The sections may not even cross at the center of the sphere since the third postulate remains unchanged and the solution is determined for any fragment of the sphere and two arbitrary limiting elements that completely enclose an inner volume in the void (Figures 16 and 17). Possible inter-reflections between the three involved surfaces are addressed in Appendix A [41,42].

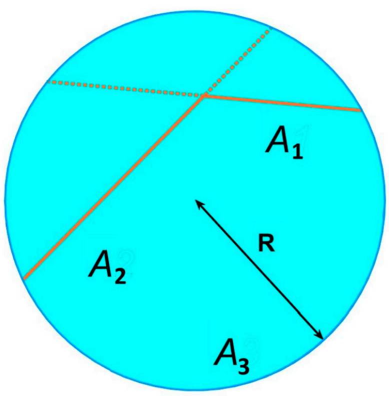

Figure 16. Side view of the surfaces A_1 and A_2 (in orange), and A_3 (in cyan) contained in a whole sphere with radius R.

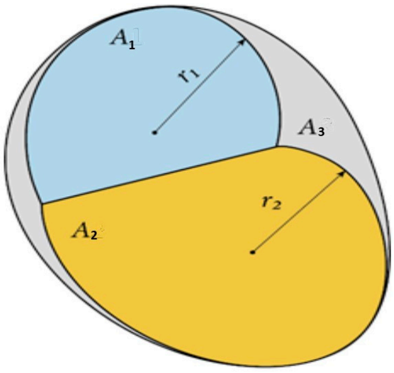

Figure 17. Front perspective of two segments A_1 and A_2 with respective radiuses r_1 and r_2, which contain A_3 (part of the sphere).

5. Conclusions

In summary, we have identified a new and significant postulate, the third principle of Cabeza-Lainez, that solves most of the problems of radiative heat transfer that appear in the interior of spheres in the absence of gases. It is not strictly necessary that the surfaces that define the selected volume within the sphere are planar, they may be curved as long as they are linked to the circles described above and, consequently, their respective self-factors, named F_{ii}, are known by virtue of Cabeza-Lainez's first principle. Subsequently, the other factors attached to the new curved boundary surfaces can be deduced by means of the second postulate, also enunciated in the article, to obtain the important fourth and fifth principles.

Spherical contour elements have been employed in all kinds of industries and building features for centuries. Nevertheless, a systematic procedure to introduce them in the heat transfer realm had not been feasible due to the many unknowns and calculation hindrances that they present. Ray-tracing or Monte Carlo simulation procedures could not manage the issues posed by curvature and/or fragmentation. With this article, we resolved the matter completely, introducing the three new and original postulates developed by the author. All axioms are related to the first principle of Cabeza-Lainez, applicable to spheres, where integral calculus is seldom required. The fundamental advances that the postulates represent lie in the fact that, being direct formulations, they can be built into new routines of algorithms for computer simulations as explained in the literature below. We have demonstrated in the references that they accommodate a great number of applications in the near future for previously ignored situations of radiative energy such as lighting technologies, aerospace fabrication, and the building sector.

In nuclear facilities, the radiative exchanges happening inside curve-shaped reactors, parts, and containers were largely unknown prior to the author's contribution and, as we know, lately they are becoming critical to ascertain in the hazardous events of maintenance and sundry incidents.

In this manner, paramount problems of the transmission and interchange of radiation can be addressed by virtue of a simple and elegant operation. All in all, we deem that the findings presented thereof should become a crucial development for the evolution of the complex, though ever-present, realm of radiative heat transfer.

Funding: This research received no external funding.

Institutional Review Board Statement: Not applicable.

Informed Consent Statement: Not applicable.

Data Availability Statement: Not applicable.

Acknowledgments: The author wants to acknowledge the help and momentum of Francisco Salguero Andujar. I recognize Encarnación Abajo Casado for being extremely supportive of my mathematical investigations. Raul Limon has been instrumental in diffusing these findings. I would like to thank Francisco J. Guevara García and Carlos Rubio Bellido for their kindness in allowing me to present the work at an early phase. Scenography of the pool at Strauss' opera Salome has been a powerful source of inspiration.

Conflicts of Interest: The authors declare no conflict of interest.

Nomenclature

E_1 and E_2 are the amounts of energy (in W/m^2) emitted in Lambertian mode by elements 1 and 2. θ_1 and θ_2 represent the angles (in radians) formed by the normals to the unit area elements of areas dA_1 and dA_2. r_{12} is the arbitrary vector (in metres) that connects the surfaces dA_1 and dA_2.

Appendix A

In the particular situation of analyzing a curved space made by three surfaces, by virtue of the third postulate presented we may need to supplement the radiative balance by considering the possible internal reflections between the said surfaces. Such an issue has been addressed by the author with the ensuing deductions [13,31]:

The final balance of energy is based on the expression:

$$E_{tot} = E_{dir} + E_{ref} \tag{A1}$$

In it, E_{dir} stands for the ratio of directly emitted energy and E_{ref} represents the amount of reflected energy. Adding both magnitudes, we find the total balance of radiated energy E_{tot}.

When more than two surfaces appear in the process of reflection, it is customary to arrange the set of necessary equations into an array. Two types of square matrices are instrumental, they are named F_r and F_d [3,31], the number of rows and columns coincides with the surfaces involved in the calculation:

$$F_d = \begin{pmatrix} 0 & F_{12}\rho_2 & F_{13}\rho_3 \\ F_{21}\rho_1 & 0 & F_{23}\rho_3 \\ F_{31}\rho_1 & F_{32}\rho_2 & F_{33}\rho_3 \end{pmatrix} \tag{A2}$$

$$F_r = \begin{pmatrix} 1 & -F_{12}\rho_2 & -F_{13}\rho_3 \\ -F_{21}\rho_1 & 1 & -F_{23}\rho_3 \\ -F_{31}\rho_1 & -F_{32}\rho_2 & 1 \end{pmatrix} \tag{A3}$$

Factors F_{ij} have been previously found, they give the energy emission exchanged by the surfaces under consideration. In this case, ρ_i stands for the ratio of reflection associated with a given surface i [3,13].

Notice, in the array defined as F_d (Equation (A2)), the last coefficient of the diagonal is non-zero since the F_{ii} factors or self-factors for the coincidental sub-indexes have definite values for curved surfaces such as the sphere, unlike cuboids or planar faces [2].

Once we are able to obtain the value of the elements in the matrices (2) and (3), we can find different formulas (Equations (A4)–(A6)) to link the direct radiation with that given by reflection [1].

$$F_r E_{ref} = F_d\, E_{dir} \tag{A4}$$

$$F_{rd} = F_r^{-1} F_d \tag{A5}$$

$$E_{ref} = F_{rd} E_{dir} \tag{A6}$$

In this manner, the issue of radiative energy interchanges in the void for curved spaces is eventually settled.

References

1. Holman, J.P. *Heat Transfer*, 7th ed.; Mac Graw Hill: Bogotá, Colombia, 1995.
2. Cabeza-Lainez, J. *Fundamentals of Luminous Radiative Transfer: An Application to the History and Theory of Architectural Design*; Crowley Editions: Seville, Spain, 2006.
3. Moon, P.H.; Spencer, D.E. *The Photic Field*; The MIT Press: Cambridge, MA, USA, 1981.
4. Orzechowski, T.; Wciślik, S. Evaporation of the Leidenfrost Droplet Located on a Thin Metal Foil. *Procedia Eng.* **2016**, *157*, 131–138. [CrossRef]
5. Wciślik, S. Thermal infrared mapping of the Leidenfrost drop evaporation. *J. Phys. Conf. Ser.* **2016**, *745*, 032064. [CrossRef]
6. Subramaniam, S.; Hoffmann, S.; Thyageswaran, S.; Ward, G. Calculation of View Factors for Building Simulations with an Open-Source Raytracing Tool. *Appl. Sci.* **2022**, *12*, 2768. [CrossRef]
7. Modest, M.F. View Factors. In *Radiative Heat Transfer*, 3rd ed.; Academic Press: Cambridge, MA, USA, 2013; pp. 129–159.
8. Hensen, J.L.M.; Lamberts, R. *Building Performance Simulation for Design and Operation*, 2nd ed.; Routledge: London, UK, 2019; ISBN 9781138392199.
9. Moon, P.H. *The Scientific Basis of Illuminating Engineering*; McGraw-Hill Book Co. Dover Publications: New York, NY, USA, 1963.
10. Howell, J.R.; Siegel, R.; Mengüç, M.P. *Thermal Radiation Heat Transfer*, 5th ed.; Taylor and Francis/CRC: New York, NY, USA, 2010.
11. Hamilton, D.C.; Morgan, W. Radiant-Interchange Configuration Factors. NASA. 1952. Available online: https://ntrs.nasa.gov/citations/19930083529 (accessed on 9 May 2023).
12. Schröder, P.; Hanrahan, P. On the Form Factor between Two Polygons. In Proceedings of the SIGGRAPH93: 20th Annual Conference and Exhibition on Computer Graphics and Interactive Techniques, Anaheim, CA, USA, 2–6 August 1993; pp. 163–164. [CrossRef]
13. Cabeza-Lainez, J. New configuration factors for curved surfaces. *J. Quant. Spectrosc. Radiat. Transf.* **2013**, *111*, 71–80. [CrossRef]
14. Lambert, J.H. *Photometria, Sive de Mensura et Gradibus Luminis, Colorum et Umbrae*; DiLaura, D., Ed.; IESNA: New York, NY, USA, 2001; p. 1764.
15. Hilbert, D.; Cohn-Vossen, S. *Geometry and the Imagination*; AMS (American Mathematical Society) Chelsea Publishing: Providence, RI, USA, 1990.
16. A Catalogue of Radiation Heat Transfer Configuration Factors. Howell, J.R. University of Texas at Austin. Available online: http://www.thermalradiation.net/indexCat.html (accessed on 23 May 2023).
17. Cabeza Lainez, J. Scientific designs of sky-lights. In Proceedings of the Conference on Passive and Low Energy Architecture (PLEA), Brisbane, Australia, 22–24 September 1999.
18. Howell, J.R. A Catalogue of Radiation Heat Transfer Configuration Factors. Factor C-43b. Available online: http://www.thermalradiation.net/sectionc/C-43b.html (accessed on 14 March 2022).
19. Howell, J.R. A Catalogue, Factor C-140b. Available online: http://www.thermalradiation.net/sectionc/C-140b.html (accessed on 10 September 2022).
20. Cabeza Lainez, J. Solar Radiation in Buildings. Transfer and Simulation Procedures. In *Solar Radiation*; Babatunde, E.B., Ed.; Chapter 16; InTech: New York, NY, USA, 2012; ISBN 978-953-51-0384-4. Available online: https://www.intechopen.com/chapters/33356 (accessed on 27 November 2022).
21. Howell, J.R.; Siegel, R.; Pinar, M.M. Radiative transfer configuration factor catalogue: A listing of relations for common geometries. *J. Quanti. Spectrosc. Radiat. Transf.* **2011**, *112*, 910–912. [CrossRef]
22. Gershun. The Light Field (translated from Russian by P. Moon and G. Timoshenko). *J. Math. Phys. Apr.* **1939**, *18*. [CrossRef]
23. Fock, V. Zur Berechnung der Beleuchtungsstärke; Optisches Institut: St. Petersburg, Russia. *Z. Phys.* **1924**, *28*, 102–113. [CrossRef]
24. Feingold, A. A new look at radiation configuration factors between disks. *J. Heat Transfer.* **1978**, *100*, 742–744. [CrossRef]
25. Cabeza-Lainez, J.M.; Pulido-Arcas, J.A. New Configuration Factor between a Circle, a Sphere and a Differential Area al Random Positions. *J. Quant. Spectrosc. Radiat. Transf.* **2013**, *129*, 272–276. [CrossRef]
26. Cabeza-Lainez, J.M.; Rodriguez-Cunill, I. The Problem of Lighting in Underground Domes, Vaults, and Tunnel-Like Structures of Antiquity; An Application to the Sustainability of Prominent Asian Heritage (India, Korea, China). *Sustainability* **2019**, *11*, 5865. [CrossRef]
27. Cabeza-Lainez, J.M.; Rodríguez-Cunill, I. Prevention of Hazards Induced by a Radiation Fireball through Computational Geometry and Parametric Design. *Mathematics* **2022**, *10*, 387. [CrossRef]
28. Faulkner, T.E. *Projective Geometry*; Dover Publications: New York, NY, USA, 2016; ISBN 978-0-486-45326-2.
29. Howell, J.R. A Catalogue of Radiation Heat Transfer Configuration Factors. Factor C-43a. Available online: http://www.thermalradiation.net/sectionc/C-43a.html (accessed on 9 November 2021).
30. Salguero-Andujar, F.; Cabeza-Lainez, J.-M. New Computational Geometry Methods Applied to Solve Complex Problems of Radiative Transfer. *Mathematics* **2020**, *8*, 2176. [CrossRef]
31. Nußelt, W. Graphische Bestimmung des Winkelverhältnisses bei der Wärmestrahlung. *Z. Ver. Dtsch. Ing.* **1928**, *72*, 673.
32. Naraghi, M.H.N. Radiation View Factors from Differential plane sources to disks- A general formulation. *Tech. Notes Am. Inst. Aeronaut. Astronaut. J.* **1988**, *2*, 3. [CrossRef]
33. MacAllister, A.S. Graphical solutions of problems involving plane surface lighting sources. *Light. World* **1911**, *56*, 135.
34. Cabeza Lainez, J.M.; Pulido Arcas, J.A.; Bellido, C.R.; Bonilla Martínez, J.M. Radiative Heat Transfer for Curvilinear Surfaces. In *Solar Radiation Applications*; Chapter 1; InTech: London, UK, 2015.

35. Howell, J.R. A Catalogue, Factor C-140a. Available online: http://www.thermalradiation.net/sectionc/C-140a.html (accessed on 13 July 2022).
36. Howell, J.R. A Catalogue, Factor C-140c. Available online: http://www.thermalradiation.net/sectionc/C-140c.html (accessed on 14 July 2022).
37. Howell, J.R. A Catalogue, Factor C-140d. Available online: http://www.thermalradiation.net/sectionc/C-140d.html (accessed on 21 September 2021).
38. DiLaura, D.L. *New Procedures for Calculating Diffuse and Non-Diffuse Radiative Exchange Form Factors*; ASME: New York, NY, USA, 1999.
39. Naraghi, M.H.N. Radiative View Factors from Spherical Segments to Planar Surfaces. *J. Thermophys. Heat Transf.* **1988**, *2*, 373–375. [CrossRef]
40. Chung, B.T.F.; Naraghi, M.H.N. Some Exact Solutions for Radiation View Factors from Spheres. *AIAA J.* **1981**, *19*, 1077–1081. [CrossRef]
41. Sasaki, K.; Sznajder, M. Analytical view factor solutions of a spherical cap from an infinitesimal surface. *Int. J. Heat Mass Transf.* **2020**, *163*, 120477. [CrossRef]
42. Cabeza-Lainez, J. Architectural Characteristics of Different Configurations Based on New Geometric Determinations for the Conoid. *Buildings* **2022**, *12*, 10. [CrossRef]